



HAL
open science

Precession due to a close binary system: an alternative explanation for ν -Octantis?

M. Morais, A. Correia

► **To cite this version:**

M. Morais, A. Correia. Precession due to a close binary system: an alternative explanation for ν -Octantis?. *Monthly Notices of the Royal Astronomical Society*, 2012, 419 (4), pp.3447-3456. 10.1111/j.1365-2966.2011.19986.x . hal-02873340

HAL Id: hal-02873340

<https://hal.science/hal-02873340>

Submitted on 1 Sep 2023

HAL is a multi-disciplinary open access archive for the deposit and dissemination of scientific research documents, whether they are published or not. The documents may come from teaching and research institutions in France or abroad, or from public or private research centers.

L'archive ouverte pluridisciplinaire **HAL**, est destinée au dépôt et à la diffusion de documents scientifiques de niveau recherche, publiés ou non, émanant des établissements d'enseignement et de recherche français ou étrangers, des laboratoires publics ou privés.

Precession due to a close binary system: an alternative explanation for ν -Octantis?

M. H. M. Morais¹* and A. C. M. Correia^{1,2}*

¹*Department of Physics, I3N, University of Aveiro, Campus Universitário de Santiago, 3810-193 Aveiro, Portugal*

²*Astronomie et Systèmes Dynamiques, IMCCE-CNRS UMR 8028, 77 Avenue Denfert-Rochereau, 75014 Paris, France*

Accepted 2011 October 11. Received 2011 October 1; in original form 2011 July 25

ABSTRACT

We model the secular evolution of a star's orbit when it has a nearby binary system. We assume a hierarchical triple system where the inter-binary distance is small in comparison with the distance to the star. We show that the major secular effect is precession of the star's orbit around the binary system's centre of mass. We explain how we can obtain this precession rate from the star's radial velocity data, and thus infer the binary system's parameters. We show that the secular effect of a nearby binary system on the star's radial velocity can sometimes mimic a planet. We analyse the radial velocity data for ν -Octantis A which has a nearby companion (ν -Octantis B) and we obtain retrograde precession of $-0:86 \pm 0:02 \text{ yr}^{-1}$. We show that if ν -Octantis B was itself a double star, it could mimic a signal with similarities to that previously identified as a planet of ν -Octantis A. Nevertheless, we need more observations in order to decide in favour of the double-star hypothesis.

Key words: methods: analytical – techniques: radial velocities – celestial mechanics – planets and satellites: detection – planets and satellites: dynamical evolution and stability – binaries: spectroscopic.

1 INTRODUCTION

Most of the extra-solar planet detections rely on measuring the parent star's wobble which is assumed to be caused by a planet. However, other effects can cause stellar wobble; thus, it is important to study these in order to avoid erroneous new planet announcements, as has already happened in the past (Queloz et al. 2001; Santos et al. 2002).

In previous articles (Morais & Correia 2008, 2011), we studied the short-term effect of a binary system on a star's motion. We noted that this could mimic a planetary companion to the star under some circumstances. In these articles, we considered moderately close binary systems (≥ 10 au) in which the star's motion around the binary's centre of mass had periods of several decades. Moreover, we realistically assumed that we had observational data for only a fraction of this period, and not several orbits.

Here, we will present another scenario that requires a different analysis. We consider a star with a close binary system (< 5 au) and assume that the observational data cover a few periods of the star's motion around the binary system's centre of mass. We will show that, in this case, we have to take into account secular effects which lead to slow precession of the star's orbit.

In Section 2 we present the secular theory for hierarchical triple star systems composed of a star and a nearby binary. In Section 3,

we show how we can measure the secular precession of the star's orbit from radial velocity data and how we can predict the binary system's parameters from this measurement. In Section 4, we apply the results from previous sections to fictitious hierarchical triple star systems. In Section 5, we discuss the reported finding of a planet in the binary system ν -Octantis. In Section 6, we present our conclusions.

2 SECULAR THEORY FOR HIERARCHICAL TRIPLE STAR SYSTEMS

We consider a triple star system composed of an observed star, m_2 , and a nearby binary of masses m_0 and m_1 . We use the Jacobi coordinates \mathbf{r}_1 (distance of m_1 to m_0) and \mathbf{r}_2 (distance of m_2 to the centre of mass of m_0 and m_1). Moreover, we assume that $|\mathbf{r}_1| \ll |\mathbf{r}_2|$ (hierarchical triple system).

2.1 Secular Hamiltonian

The Hamiltonian is (Lee & Peale 2003; Farago & Laskar 2010)

$$H = -\frac{\mathcal{G}m_0m_1}{2a_1} - \frac{\mathcal{G}(m_0 + m_1)m_2}{2a_2} + F, \quad (1)$$

where the first term describes the Keplerian motion of m_1 with respect to m_0 (inner binary), the second term describes the Keplerian motion of m_2 with respect to the centre of mass of m_0 and m_1 (outer

*E-mail: helena.morais@ua.pt (MHMM); correia@ua.pt (ACMC)

binary), and

$$F = -\mathcal{G}m_0m_2 \left(\frac{1}{r_{02}} - \frac{1}{r_2} \right) - \mathcal{G}m_1m_2 \left(\frac{1}{r_{12}} - \frac{1}{r_2} \right), \quad (2)$$

where \mathcal{G} is the gravitational constant, the distance of m_2 to m_0 is

$$r_{02} = r_2 + \frac{m_1}{m_0 + m_1} r_1, \quad (3)$$

and the distance of m_2 to m_1 is

$$r_{12} = r_2 - \frac{m_0}{m_0 + m_1} r_1. \quad (4)$$

Expanding $1/r_{02}$ and $1/r_{12}$ in powers of $\rho = r_1/r_2$ and retaining terms up to the order of ρ^2 , we obtain the quadrupole Hamiltonian

$$F = -\frac{\mathcal{G}m_2}{r_2} \frac{m_0m_1}{m_0 + m_1} \frac{\rho^2}{2} (3(\hat{r}_1 \cdot \hat{r}_2)^2 - 1), \quad (5)$$

where \hat{r}_1 and \hat{r}_2 are the versors of r_1 and r_2 , respectively.

The secular quadrupole Hamiltonian is obtained by averaging equation (5) with respect to the inner and outer binaries' orbital periods (Frago & Laskar 2010)

$$\bar{F} = C [2 - 12e_1^2 - 6(1 - e_1^2)(\hat{k}_1 \cdot \hat{k}_2)^2 + 30e_1^2(\hat{i}_1 \cdot \hat{k}_2)^2], \quad (6)$$

where

$$C = \frac{\mathcal{G}}{16} \frac{m_0m_1}{m_0 + m_1} \frac{m_2}{(1 - e_2^2)^{3/2}} \frac{a_1^2}{a_2^3}, \quad (7)$$

\hat{k}_2 and \hat{k}_1 are, respectively, the versors of the angular momentum vectors of the outer binary (G_2) and inner binary (G_1), and \hat{i}_1 is the unit vector in the inner binary's orbital plane that points towards the inner binary's pericentre.

In an arbitrary reference frame, we have

$$\hat{k}_1 \cdot \hat{k}_2 = \sin I_1 \sin I_2 \cos(\Omega_1 - \Omega_2) + \cos I_1 \cos I_2, \quad (8)$$

$$\begin{aligned} \hat{i}_1 \cdot \hat{k}_2 &= -\sin I_2 \cos I_1 \sin \omega_1 \cos(\Omega_1 - \Omega_2) \\ &\quad - \sin I_2 \cos \omega_1 \sin(\Omega_1 - \Omega_2) \\ &\quad + \sin I_1 \sin \omega_1 \cos I_2, \end{aligned} \quad (9)$$

where I_1 is the inner binary's inclination, I_2 is the outer binary's inclination, Ω_1 is the inner binary's longitude of ascending node, Ω_2 is the outer binary's longitude of ascending node, and ω_1 is the inner binary's argument of pericentre.

Kozai (1962), Krymowski & Mazeh (1999) and Ford, Kozinsky & Rasio (2000) write the Hamiltonian in the invariant plane reference frame (Fig. 1). In this reference frame, $\Omega_1 - \Omega_2 = 180^\circ$, and the relative inclination is $i = I_1 + I_2$; thus,

$$\bar{F} = C [(2 + 3e_1^2)(3 \cos^2 i - 1) + 15e_1^2 \sin^2 i \cos(2\omega_1)] \quad (10)$$

and due to conservation of angular momentum

$$G^2 = G_1^2 + G_2^2 + 2G_1G_2 \cos i = \text{const.} \quad (11)$$

2.2 Secular equations

The Delaunay canonical variables for this triple system are the angles l_j (mean anomalies), ω_j (arguments of pericentre), Ω_j (longitudes of ascending nodes) and their conjugate momenta, respectively,

$$L_j = \beta_j \sqrt{\mu_j a_j}, \quad (12)$$

$$G_j = L_j \sqrt{1 - e_j^2}, \quad (13)$$

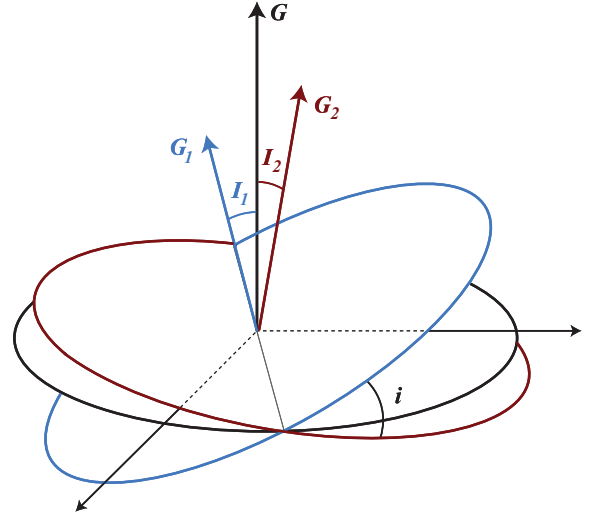


Figure 1. The invariant plane is orthogonal to the total angular momentum vector $G = G_1 + G_2$, where G_2 and G_1 are, respectively, the angular momentum vectors of the outer and inner binaries.

$$H_j = G_j \cos I_j, \quad (14)$$

with $j = 1$ (inner binary) and $j = 2$ (outer binary),

$$\beta_1 = \frac{m_0m_1}{m_0 + m_1}, \quad (15)$$

$$\beta_2 = \frac{m_2(m_0 + m_1)}{m_0 + m_1 + m_2}, \quad (16)$$

$$\mu_1 = \mathcal{G}(m_0 + m_1) \text{ and } \mu_2 = \mathcal{G}(m_0 + m_1 + m_2).$$

By definition, the secular Hamiltonian does not depend on the mean anomalies, l_j ; hence, their conjugate momenta, L_j , and thus the semimajor axes, a_j , are constant. The secular evolution is obtained from

$$\dot{G}_j = \frac{\partial \bar{F}}{\partial \omega_j}, \quad (17)$$

$$\dot{\omega}_j = -\frac{\partial \bar{F}}{\partial G_j}, \quad (18)$$

$$\dot{H}_j = \frac{\partial \bar{F}}{\partial \Omega_j}, \quad (19)$$

$$\dot{\Omega}_j = -\frac{\partial \bar{F}}{\partial H_j}. \quad (20)$$

The quadrupole Hamiltonian (equation 6) does not depend on ω_2 , hence, from equation (17) with $j = 2$, G_2 and e_2 are constant.

Kozai (1962) and Kinoshita & Nakai (2007) derived expressions for the secular evolution of the inner binary in the limit $m_1 = 0$ (inner restricted problem), using the quadrupole Hamiltonian. In this case, the outer binary's orbit coincides exactly with the invariant plane which is the natural choice of reference frame. The Hamiltonian is given by equation (10)¹ and the secular evolution of the inner binary, i.e. (e_1, ω_1) , is given by equations (17) and (18) with

¹ When $m_1 = 0$, we must replace $\beta_1 = 1$ (equation 15) into equation (7) (Kozai 1962). Note that there is a mistake in the expression given in Kinoshita & Nakai (2007) since it should have a_1^2 and not a_2^2 in the nominator.

$j = 1$. Moreover, the secular oscillations of e_1 and i are coupled due to conservation of angular momentum (equation 11).²

Following Kozai (1962) and Kinoshita & Nakai (2007), we will describe the secular dynamics of prograde orbits ($0^\circ < i < 90^\circ$) but since equation (10) is invariant with respect to the transformation $i \rightarrow 180^\circ - i$, the secular dynamics is the same for prograde (inclination i) or retrograde (inclination $180^\circ - i$) orbits. When $0^\circ < i < i_c \approx 40^\circ$, ω_1 circulates while the eccentricity, e_1 , and relative inclination, i , exhibit secular oscillations with amplitude that increases with the relative inclination (in particular, coplanar orbits keep constant eccentricity, e_1). When $i > i_c \approx 40^\circ$, there are stationary solutions ($i = \text{const}$, $e_1 = \sqrt{1 - (5/3)\cos^2 i} = \text{const}$, $\omega_1 = \pm 90^\circ$), and Kozai cycles where i , e_1 and ω_1 oscillate around the stationary solutions.

Farago & Laskar (2010) showed that the secular motion of the inner binary when $0^\circ \leq i \leq 90^\circ$ (prograde orbits) is, in the general problem ($m_1 \neq 0$), equivalent to the inner restricted problem ($m_1 = 0$), as long as

$$G_1^2 - L_1^2 + 4G_2^2 + 2G_1G_2 \cos i > 0. \quad (21)$$

Defining $X = L_2/L_1$, we can write equation (21) as

$$4(1 - e_2^2)X^2 + 2X\sqrt{1 - e_1^2}\sqrt{1 - e_2^2}\cos i - e_1^2 > 0. \quad (22)$$

The left-hand side of equation (22) is a second-degree polynomial in X which is a convex function with two roots $X_1 < 0$ and $5/2 \geq X_2 > X_1$. Therefore, inequality (equation 21) is verified if $L_1/L_2 < 2/5$, which is generally true if $a_1/a_2 \ll 1$ (hierarchical system) unless $m_0 + m_1 \gg m_2$.

Equations (17) and (18) with $j = 2$ describe the secular evolution of the outer binary's eccentricity and argument of pericentre. We noted that the secular quadrupole Hamiltonian (equation 6) does not depend on ω_2 ; hence, from equation (17) with $j = 2$, the conjugate momentum, G_2 , and thus the eccentricity, e_2 , are constant. From equation (18) with $j = 2$, we obtain the outer binary pericentre's precession rate

$$\dot{\omega}_2 = \frac{12C}{G_2} \left[\frac{1}{2} - 3e_1^2 - \frac{3}{2}(1 - e_1^2)(\hat{k}_1 \cdot \hat{k}_2)^2 + \frac{15}{2}e_1^2(\hat{i}_1 \cdot \hat{k}_2)^2 \right]. \quad (23)$$

Higher order secular octupole terms cause long-term small-amplitude oscillations in e_1 and e_2 , which are more important for small to moderate values of the relative inclination, i (Krymowski & Mazeh 1999; Ford et al. 2000; Lee & Peale 2003).

2.3 Precession of the outer binary's orbit

The outer binary's precession rate (equation 23) depends on the secular motion of the inner binary. Moreover, in the invariant reference frame (Fig. 1) we have

$$G_1 \sin I_1 = G_2 \sin I_2. \quad (24)$$

Since $a_1 \ll a_2$ (hierarchical system) then, in general, $G_1 \ll G_2$ (unless $m_0 + m_1 \gg m_2$); thus, $\sin I_2 \ll 1$, i.e. the outer binary's motion coincides approximately with the invariant plane. Therefore, we express the right-hand side of equation (23) using the reference plane of the outer binary's orbit, i.e. setting $I_2 = 0$ and $I_1 = i$ in equations (8) and (9), thus obtaining

$$\dot{\omega}_2 \approx \frac{12C}{G_2} A, \quad (25)$$

² Since $G^2 = G_1^2 + G_2^2 + 2G_1G_2 \cos i = \text{const}$, $G_2 = \text{const}$ and $G_1 \ll G_2$; hence $(1 - e_1^2)\cos^2 i \approx \text{const}$.

$$A = \left(\frac{1}{2} + \frac{3}{4}e_1^2 \right) (3\theta^2 - 1) + \frac{15}{4}e_1^2(1 - \theta^2)\cos(2\omega_1), \quad (26)$$

where $\theta = \cos i$.

Equation (25) is an approximation of the precession rate, $\dot{\omega}_2$, because the outer binary's orbit is not fixed but exhibits small-amplitude oscillations around the invariant plane. The angle ω_1 on the right-hand side of equation (26) is measured with respect to the outer binary's orbit or, equivalently, with respect to the invariant plane.³ This formulation is necessary in order to describe the motion of the inner binary (Kozai 1962; Kinoshita & Nakai 2007; Farago & Laskar 2010). However, the angle ω_2 represents the location of the outer binary's periape with respect to the intersection with the observer's plane (when dealing with radial velocity data, this is the plane orthogonal to the line of sight).

The long-term evolution of Kozai cycles (which exist if $i > i_c \approx 40^\circ$) was investigated by Eggleton & Kiseleva-Eggleton (2001), Fabrycky & Tremaine (2007) and Wu, Murray & Ramsahai (2007). Typically, if e_1 becomes close to unity during a Kozai cycle, a combination of tidal evolution and relativistic effects will eventually disrupt the Kozai cycle and freeze the relative inclination, i . This will be followed by tidal damping of the semimajor axis, a_1 , and eccentricity, e_1 . The end state of a Kozai cycle that reaches $e_1 \approx 1$ will be a tighter inner binary (smaller $\alpha = a_1/a_2$) on a circular orbit. Obviously, if $\alpha \ll 1$ then, as $\dot{\omega}_2 \propto \alpha^2 n_2$, the precession of the outer binary's orbit will be slow, thus difficult to detect from observational data. On the other hand, orbits near the Kozai stationary solution are less prone to undergo tidal evolution and should keep the original value of α .

We will, therefore, assume three scenarios for the inner binary's motion in the invariant plane reference frame.

(i) $i < i_c$ where \bar{e}_1 and $\bar{\theta}$ are average values of the secular oscillations in e_1 and θ , respectively. If $e_1 \neq 0$, then ω_1 circulates and we have, on average, $\bar{A} = (1/2 + 3\bar{e}_1^2/4)(3\bar{\theta}^2 - 1)$. If $e_1 \approx 0$, then $A \approx (3\theta^2 - 1)/2$.

(ii) $i > i_c$ but the inner binary's orbit was initially a high-amplitude Kozai cycle that was circularized by tidal damping. In this case we also have $A = (3\theta^2 - 1)/2$.

(iii) $i > i_c$ and the inner binary is at the Kozai stationary solution with $\omega_1 = \pm 90^\circ$ and $\theta^2 = 3(1 - e_1^2)/5$. In this case, $A = -5(2\theta^2 - 1)(\theta^2 - 1)$.

In all scenarios above, the precession rate $\dot{\omega}_2$ is approximately constant.

In Fig. 2 we plot the normalized precession rate, A , given by equation (26), when $e_1 = 0$ and at the Kozai stationary solution. We see that when $e_1 = 0$, precession is prograde when $i < 54.73^\circ$ and retrograde when $i > 54.73^\circ$. At the Kozai stationary solution, which exists only when $i > i_c \approx 40^\circ$, precession is retrograde when $i > 45^\circ$.

Fig. 2 shows the normalized precession rate, A , for $0^\circ < i < 90^\circ$ (prograde orbits). However, we noted previously that equation (10) is invariant with respect to the transformation $i \rightarrow 180^\circ - i$; hence, the precession rate (equation 26) is the same for prograde (inclination i) or retrograde (inclination $180^\circ - i$) orbits.

We performed numerical integrations of the equations of motion of hierarchical triple star systems with parameters $m_2 = M_\odot$, $a_2 = 3.0$ au, $e_2 = 0.2$, and initial angles $I_2 = 0^\circ$, $\Omega_1 = \Omega_2$ and

³ Since the intersection of the inner and outer binaries' orbits (line of nodes) is in the invariant plane (Fig. 1), then the angle ω_1 is the same when measured with respect to either the outer binary's orbit or the invariant plane.

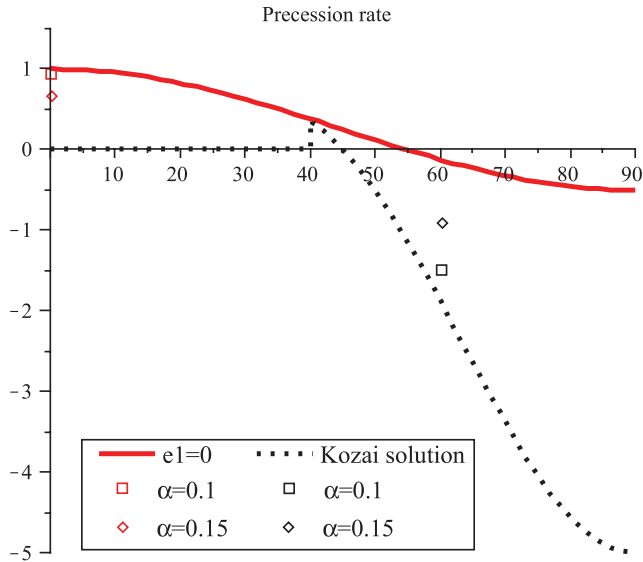


Figure 2. Comparison between theoretical precession rates (A given by equation 26) and values obtained in simulations.

$\omega_1 = 90^\circ$. The inner binary had $m_1 = 0.08 M_\odot$ and $m_0 = 0.42 M_\odot$, semimajor axial ratio $\alpha = a_1/a_2$. We chose two configurations: (i) $i = 0$ and $e_1 = 0.01$ (coplanar nearly circular orbit), and (ii) $i = 60^\circ$ and $e_1 = 0.76$ (Kozai stationary solution). In Fig. 2 we show the comparison between the theoretical precession rates and the values obtained in the simulations (up to 100 yr). We see that the quadrupole approximation becomes less accurate when we increase the semimajor axial ratio α . This could be either due to truncation of the Hamiltonian at order α^2 or due to inaccuracies of the first-order secular theory (Giuppone et al. 2011). These results do not vary much with other choices for the masses m_0 and m_1 , as long as $m_b = m_0 + m_1$ is kept constant.

3 ORBITAL PRECESSION IN RADIAL VELOCITY DATA

3.1 Measuring precession rates

The radial velocity of a star, m_2 , with a close binary system, $m_b = m_0 + m_1$, is approximately

$$V_r = V_{r0} + V_{rst}, \quad (27)$$

where V_{rst} are short-period perturbation terms obtained in Morais & Correia (2011),

$$V_{r0} = K [\cos(f_2 + \omega_2) + e_2 \cos(\omega_2)], \quad (28)$$

with

$$K = \frac{n_2 a_2}{\sqrt{1 - e_2^2}} \frac{m_b}{m_2 + m_b} \sin I_2, \quad (29)$$

and we assume that ω_2 changes linearly with time (Section 2.3), i.e.

$$\omega_2 = \omega_{20} + \dot{\omega}_2 t. \quad (30)$$

The precession of the star's orbit can be inferred from the radial velocity curve mostly due to the term $\propto e_2$ in equation (28). Typically, the observation time-span, t_{obs} , is much shorter than the precession cycle, thus if $\omega_{20} \neq 0^\circ, 180^\circ$,

$$K e_2 \cos(\omega_2) \approx K e_2 [\cos(\omega_{20}) - \sin(\omega_{20}) \dot{\omega}_2 t] \quad (31)$$

with $t \leq t_{\text{obs}}$.

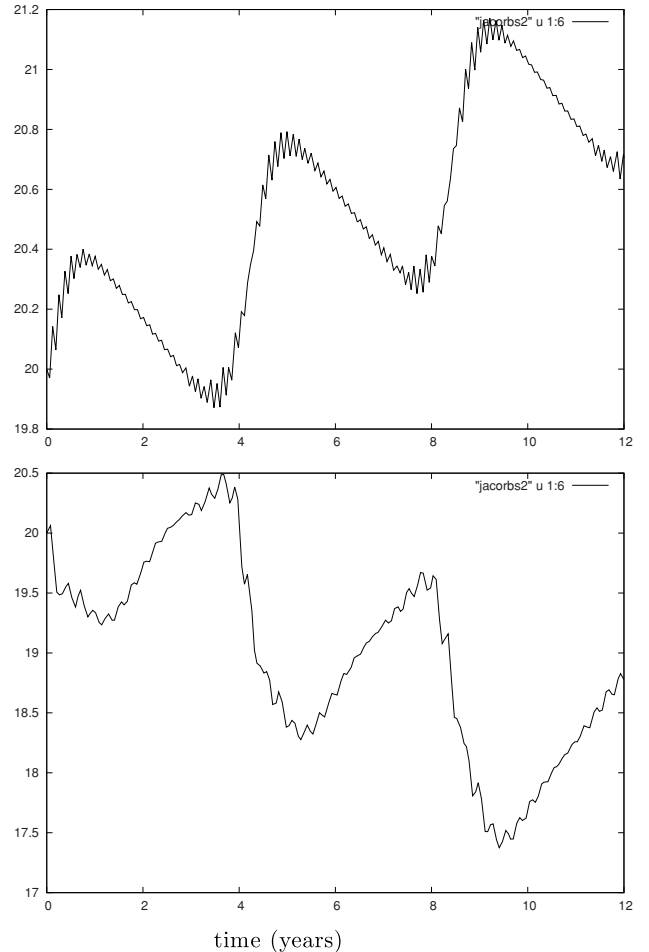


Figure 3. Evolution of angle ω_2 , showing secular drift and short-period oscillations, obtained for simulations as in Section 4.1 but without observational errors: case I (top panel) and case II (bottom panel).

Hence, equation (28) is approximately a Keplerian radial velocity curve whose amplitude has a linear drift which is at most ($\omega_{20} = 90^\circ, 270^\circ$)

$$K e_2 \dot{\omega}_2 t_{\text{obs}}. \quad (32)$$

If $\omega_{20} = 0^\circ, 180^\circ$, the radial velocity curve's amplitude has a quadratic drift $K e_2 (\dot{\omega}_2 t_{\text{obs}})^2 / 2$.

In order to measure $\dot{\omega}_2$ with accuracy, two conditions must be met. First, the drift (equation 32) must be larger than the observation's precision. Secondly, the observation time-span, t_{obs} , must be a few outer binary periods so that we can distinguish the secular drift, $\dot{\omega}_2 t_{\text{obs}}$, from short-period oscillations, $\Delta\omega$ (Morais & Correia 2011), i.e. we must have $\dot{\omega}_2 t_{\text{obs}} \gg \Delta\omega$ (see Fig. 3). These two conditions help us predict when can we measure accurately the outer binary's precession rate. However, in practice we estimate $\dot{\omega}_2$ by fitting a precessing Keplerian orbit (equations 28 and 30) to the radial velocity data.

3.2 Estimating inner binary parameters

From equation (25),

$$\dot{\omega}_2 \propto x(1-x)a_1^2 A, \quad (33)$$

where $x = m_1/m_b$, $m_b = m_0 + m_1$ and A is a function of θ (cf. Section 2.3).

Therefore, we can use the measured precession rate, $\dot{\omega}_2$, to estimate the parameters of an hidden binary (i.e. m_1 and a_1) through the quantity $x(1-x)a_1^2$. However, since A is a function of $\theta = \cos i$ which is unknown, we have to make some assumptions. From Fig. 2 we see that prograde precession is faster when $i = 0$ and that, if the inner binary is at the Kozai stationary solution, retrograde precession occurs if $i > 45^\circ$ and it is faster when $i = 90^\circ$. As orbits with high relative inclination, i , will reach values of e_1 near unity, these are likely to become unstable or undergo tidal evolution; hence, we set a maximum value of $i = 60^\circ$. Therefore, if $\dot{\omega}_2 > 0$, we assume that $i = 0$ and $e_1 = 0$; if $\dot{\omega}_2 < 0$ we assume that $i = 60^\circ$ and $e_1 = 0.76$. These assumptions imply maximum precession rates⁴ (in absolute value), thus they give us minimum estimates for the parameter $x(1-x)a_1^2$.

In order to estimate the hidden inner binary component's mass, m_1 , we must provide an estimate for the inner binary's semimajor axis, a_1 . Holman & Wiegert (1999) measured the size of stability regions around binary star components. They assume a massless particle orbiting in the binary system's plane and find that this is stable if $a_1 \leq a_c$ with

$$\begin{aligned} \frac{a_c}{a_2} = & (0.464 \pm 0.006) + (-0.380 \pm 0.010)\mu \\ & + (-0.631 \pm 0.034)e_2 + (0.586 \pm 0.061)\mu e_2 \\ & + (0.150 \pm 0.041)e_2^2 + (-0.198 \pm 0.074)\mu e_2^2, \end{aligned} \quad (34)$$

where a_2 and e_2 are, respectively, the outer binary's semimajor axis and eccentricity, and the mass parameter $\mu = m_2/(m_2 + m_b)$.

4 EXAMPLES

To test our model, we performed numerical integrations of the equation of motion of hierarchical triple systems composed of a star, m_2 , and a close-by binary, m_b . We chose masses $m_2 = M_\odot$ and $m_b = 0.5 M_\odot$, and semimajor axes $a_2 = 3$ au and $a_1 = 0.3$ au, which imply periods $T_2 = 4.24$ yr for the outer binary and $T_1 = 84.9$ d for the inner binary, and semimajor axial ratio $\alpha = a_1/a_2 = 0.1$. The initial angles were $I_2 = 90^\circ$, $\Omega_1 = \Omega_2 = 0^\circ$, $\omega_1 = 90^\circ$ and $\omega_2 = 20^\circ$. We computed the radial velocity of the star m_2 and simulated observational data points for a time-span, t_{obs} , and a certain precision limit. We then applied the traditional techniques used in radial velocity data analysis.

4.1 Measuring precession rates

To test in which circumstances we are able to measure the outer binary's precession rate, we set the outer binary on an eccentric orbit ($e_2 = 0.2$).

Case I is a coplanar triple system ($i = 0$, i.e. $I_1 = I_2 = 90^\circ$) where the inner binary has masses $m_0 = 0.42 M_\odot$ and $m_1 = 0.08 M_\odot$, and a nearly circular orbit ($e_1 = 0.01$). In Table 1 we show the results of fitting a fixed Keplerian orbit (fit 0) or a precessing Keplerian orbit (fit 1) to the data time series with 128 points over $t_{\text{obs}} \approx 8$ yr, at precisions of about 5 m s^{-1} (A) and 1 m s^{-1} (B), respectively. From Fig. 3 (top) we see that since $t_{\text{obs}} = 8$ yr, $\Delta\omega > \dot{\omega}_2 t_{\text{obs}}$. The maximum radial velocity drift over t_{obs} is 18.6 m s^{-1} . At a precision of 5.425 m s^{-1} (A), the observation error is 29 per cent of the maximum drift. Therefore, fit (1) is only slightly better than fit (0). However, at a precision of 1.085 m s^{-1} (B), the observation error is only 6 per cent

⁴ However, if $e_1 \neq 0$, the precession rate at $i = 0$ increases by a factor of $1 + 3e_1^2/2$ with respect to $e_1 = 0$.

Table 1. Fits to case I ($m_0 = 0.42 M_\odot$, $m_1 = 0.08 M_\odot$, $i = 0$ and $e_1 = 0.01$) with $t_{\text{obs}} = 8$ yr and different precisions.

Case I	Fit	A	B
Precision (m s^{-1})	–	5.425	1.085
T (d)	(1)	1544.12 ± 0.05	1544.15 ± 0.01
	(0)	1544.15 ± 0.05	1544.18 ± 0.01
K (m s^{-1})	(1)	7172.9 ± 0.7	7173.86 ± 0.13
	(0)	7172.6 ± 0.7	7173.62 ± 0.13
e	(1)	0.19879 ± 0.00009	0.19873 ± 0.00002
	(0)	0.19875 ± 0.00009	0.19870 ± 0.00002
$\dot{\omega}$ (deg yr^{-1})	(1)	0.115 ± 0.016	0.0937 ± 0.0032
$\sqrt{\chi^2}$	(1)	1.569	1.660
	(0)	1.690	3.097
rms (m s^{-1})	(1)	9.1850	1.9154
	(0)	9.8849	3.4024

of the maximum drift; thus, fit (1) is clearly better than fit (0). The theoretical value (quadrupole approximation) for the precession rate is $\dot{\omega}_2 = 0:093 \text{ yr}^{-1}$ while the true value (simulations up to 100 yr) is $\dot{\omega}_2 = 0:089 \text{ yr}^{-1}$.

Case II has an inner binary with masses $m_0 = 0.35 M_\odot$ and $m_1 = 0.15 M_\odot$, with $i = 60^\circ$ (i.e. $I_1 = 30^\circ$ and $I_2 = 90^\circ$) and $e_1 = 0.76$ (Kozai stationary solution). In Table 2 we show the results of fitting a fixed Keplerian orbit (fit 0) or a precessing Keplerian orbit (fit 1) to data time series with 99 points over $t_{\text{obs}} \approx 6$ yr (C), and to data time series with 154 points over $t_{\text{obs}} \approx 12$ yr (D), both at a precision of about 5 m s^{-1} . The maximum radial velocity drifts over 6 and 12 yr are, respectively, 31 and 62 m s^{-1} , which correspond to observation errors of, respectively, 16 and 8 per cent of the maximum drift. From Fig. 3 (bottom) we see that when $t_{\text{obs}} = 6$ yr, $\Delta\omega \approx \dot{\omega}_2 t_{\text{obs}}$ while when $t_{\text{obs}} = 12$ yr, $\Delta\omega \ll \dot{\omega}_2 t_{\text{obs}}$. Therefore, when $t_{\text{obs}} = 6$ yr (C), fit (1) is slightly better than fit (0) but when $t_{\text{obs}} = 12$ yr (D), fit (1) is clearly better than fit (0). The theoretical value (quadrupole approximation) for the precession rate is $\dot{\omega}_2 = -0:272 \text{ yr}^{-1}$ while the true value (simulations up to 100 yr) is $\dot{\omega}_2 = -0:238 \text{ yr}^{-1}$.

Table 2. Fits to Case II ($m_0 = 0.35 M_\odot$, $m_1 = 0.15 M_\odot$, $i = 60^\circ$ and $e_1 = 0.76$) with a precision of 5.4 m s^{-1} and different t_{obs} .

Case II	Fit	C	D
t_{obs} (yr)	–	6	12
T (d)	(1)	1567.74 ± 0.07	1567.75 ± 0.03
	(0)	1567.44 ± 0.07	1567.70 ± 0.03
K (m s^{-1})	(1)	7135.81 ± 0.89	7135.61 ± 0.60
	(0)	7139.36 ± 0.84	7134.50 ± 0.60
e	(1)	0.20495 ± 0.00011	0.20504 ± 0.00009
	(0)	0.20491 ± 0.00011	0.20558 ± 0.00009
$\dot{\omega}$ (deg yr^{-1})	(1)	-0.256 ± 0.021	-0.2606 ± 0.0086
$\sqrt{\chi^2}$	(1)	1.656	1.628
	(0)	2.077	2.984
rms (m s^{-1})	(1)	9.4952	9.5135
	(0)	11.6178	16.1299

Table 3. Hierarchical triple systems ($\alpha = 0.1$) with inner binary on a nearly circular orbit (if $i < 40^\circ$) or at the Kozai stationary solution (if $i > 40^\circ$): comparison between outer binary's theoretical (t) and observed (s) precession rates; $\sqrt{\chi^2}$ ratio between fit (1) and fit (0) to outer binary's orbit; minimum mass of hidden inner binary component, m_1 .

i ($^\circ$)	e_1	$\dot{\omega}_2$ (t)	$\dot{\omega}_2$ (s)	Ratio $\sqrt{\chi^2}$	m_1 (M_\odot)
0	0.01	0.0928	+0.094 ± 0.003	0.54	0.027
20	0.01	0.0765	+0.078 ± 0.003	0.60	0.022
40	0.01	0.0353	+0.040 ± 0.003	0.85	0.011
50	0.56	-0.0473	-0.040 ± 0.003	0.89	0.006
55	0.67	-0.1065	-0.099 ± 0.003	0.67	0.015
60	0.76	-0.1740	-0.167 ± 0.003	0.50	0.025

4.2 Estimating inner binary parameters

We simulated triple systems as described above with the observed star on an eccentric orbit with $e_2 = 0.2$ (outer binary) around an inner binary with masses $m_0 = 0.42 M_\odot$ and $m_1 = 0.08 M_\odot$, and semimajor axis $a_1 = 0.3$ au. The values of the relative inclination were $i = 0^\circ, 20^\circ, 40^\circ, 50^\circ, 55^\circ$ and 60° . When $i < 40^\circ$ the inner binary had a nearly circular orbit ($e_1 = 0.01$), and when $i \geq 40^\circ$ it had an eccentric orbit near the Kozai stationary solution.⁵ In all cases, $t_{\text{obs}} = 8$ yr, and the precision limit was about 1 m s^{-1} .

In Table 3 we present the precession rates (theoretical and measured in the simulations) and the ratio between $\sqrt{\chi^2}$ of fit (1) and fit (0) which measures the goodness of fit (1) with respect to fit (0). As explained in Section 3.2, we obtain minimum estimates for the inner binary parameter, $x(1-x)a_1^2$ with $x = m_1/m_b$ (equation 33), assuming $i = 0$ and $e_1 = 0$ when $\dot{\omega}_2 > 0$, or $i = 60^\circ$ and $e_1 = 0.76$ when $\dot{\omega}_2 < 0$ (cf. Fig. 2). We can then obtain minimum estimates for m_1 assuming $a_1 = a_c = 0.49$ au which is the maximum size of stable orbits (massless particle $m_1 \ll m_b$) around $m_0 \approx m_b$ in the coplanar case (see equation 34 with $e_2 = 0.2$ and $\mu = 0.67$). These estimates are all realistic (minimum mass of the hidden inner binary companion between 6 and $27 M_J$), hence can be used as input parameters for an N -body fit which can provide best choice values for m_1 and a_1 .

4.3 Can precession mimic a planet?

Here, we repeat the question already posed in Morais & Correia (2008, 2011). If we do not know about the inner binary's presence because one of its components is unresolved, can the binary's effect be mistaken as a planet?

In Morais & Correia (2008, 2011), we showed that the residuals left over from fitting a fixed Keplerian orbit to the outer binary (observed star's orbit around the inner binary's centre of mass) contained additional periodic signals that could be mistaken as planets. Here, we show an example of similar behaviour obtained from the previous simulation (case II with $t_{\text{obs}} = 6$ yr) in Fig. 4 (top). The

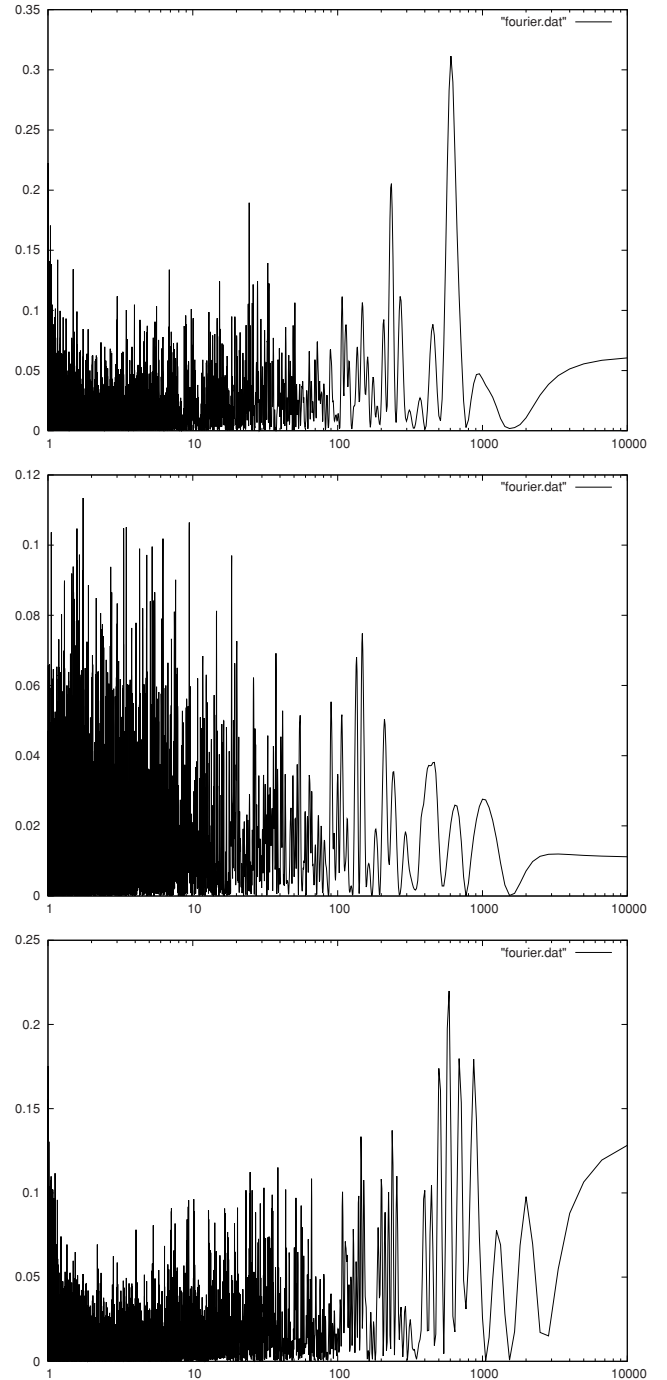


Figure 4. Periodogram of residuals after fit (0) and fit (1) to radial velocity data from the simulation in Table 2 with $t_{\text{obs}} = 6$ yr (top and middle panels, respectively) and after fit (0) to the simulation in Table 2 with $t_{\text{obs}} = 12$ yr (bottom).

periodogram⁶ has an obvious peak at 606 d, which is nearly commensurate (ratio 2/5) with the outer binary's period. However, this peak disappeared when we fitted a precessing Keplerian orbit to the outer binary (Fig. 4, middle), and it was no longer prominent

⁵ The Kozai stationary solution has $e_1 = \sqrt{1 - (5/3) \cos^2 i}$ and $\omega_1 = \pm 90^\circ$.

⁶ We compute generalized Lomb–Scargle periodograms as defined in Zechmeister & Kurster (2009).

when we increased the observation time-span to $t_{\text{obs}} = 12$ yr (Fig. 4, bottom).

In Morais & Correia (2011) we studied the short-term effect of a binary system on a nearby star in the case of eccentric and inclined orbits. We noted that, when the observed star's orbit (outer binary) was eccentric, the radial velocity was composed of a main Keplerian term that described the star's motion around the inner binary's centre of mass, and short-period terms [obtained by integrating with respect to time equation (34) in Morais & Correia (2011)]. In particular, some short-period terms appeared at harmonics of the outer binary's frequency, n_2 . However, in Morais & Correia (2011) we considered that t_{obs} was only a fraction of the outer binary's period. In this situation, the outer binary's orbit was not well constrained and these harmonics were incorporated into the main Keplerian term. Now, as t_{obs} covers a few outer binary orbits, these harmonics will appear in the residuals left over from fitting a fixed Keplerian curve to the outer binary. However, the observed star's orbit (outer binary) is, in fact, precessing and the precession rate, $\dot{\omega}_2$, is approximately constant in the long term but has short-term oscillations (see Fig. 3). If t_{obs} covers only a few outer binary orbits, these short-term oscillations will cause mixing up of the frequencies; thus, the signals do not exactly coincide with harmonics of n_2 . In particular, combinations of these harmonics can appear (Fig. 4, top). When we fit a precessing Keplerian orbit to the outer binary, as t_{obs} is short compared to the precessional period, the signals at or nearby harmonics of n_2 are incorporated into the precessing Keplerian orbit (Fig. 4, middle). As t_{obs} increases, the short-period oscillations become negligible with respect to the secular terms (Fig. 4, bottom).

If the observed star has a circular orbit, then there is no pericentre precession. When the inner binary's orbit is also circular but inclined ($i < 40^\circ$) with respect to the outer binary,⁷ the star's radial velocity is composed of a main Keplerian term (circular orbit with frequency n_2) and short-period terms [obtained by integrating with respect to time equation (21) in Morais & Correia (2011)]. In particular, there are signals at frequencies n_2 and $3n_2$. The term with frequency n_2 is simply incorporated into the main Keplerian fit. However, the term with frequency $3n_2$ can be mistaken as a planet at the 3/1 mean motion resonance with a companion 'star' of mass $m_b = m_0 + m_1$.

We simulated a triple system, as explained at the beginning of Section 4, with $m_1 = m_2 = 0.25 M_\odot$, $e_2 = 0$, $e_1 = 0$ and $i = 30^\circ$. We generated radial velocity data with 154 points over $t_{\text{obs}} = 12$ yr, at a precision of 0.543 m s^{-1} . In Fig. 5, we show a periodogram of the residuals left over after fitting a Keplerian orbit to the outer binary. As expected, we see peaks at 505 d (frequency $3n_2$, harmonic of n_2) and 46 d (frequency $2n_1 - 3n_2$, short-period term as in Morais & Correia 2008) with amplitudes 1.7 and 1.2 m s^{-1} , respectively. These can be mistaken as planets.

5 A PLANET IN ν -OCTANTIS?

The system ν -Octantis is a close single-line spectroscopic binary. Ramm et al. (2009) published radial velocity data consisting of 221 points covering a time-span of $t_{\text{obs}} = 1862$ d, with a precision of around 5 m s^{-1} (inferred from the published observation errors). Combining the radial velocity data with astrometric measurements, Ramm et al. (2009) derived improved parameters for the ν -Octantis binary (Table 4). The residuals left over from fitting a Keplerian orbit to ν -Octantis show an additional signal, which Ramm et al. (2009)

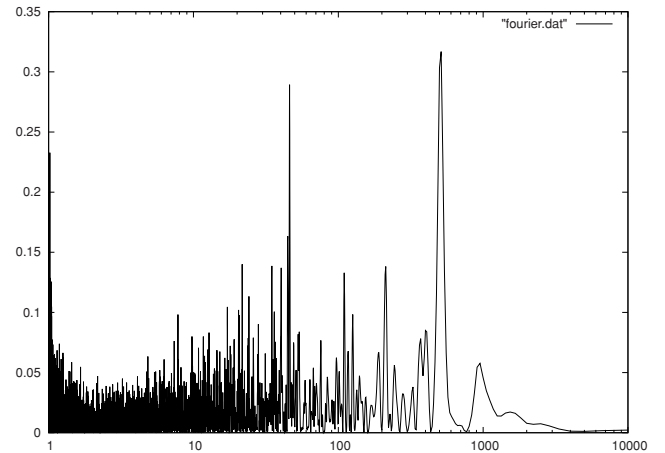


Figure 5. Periodogram of residuals after fit (0) to radial velocity data from the simulation of the circular non-coplanar triple star system composed of an observed star and a companion unresolved binary. Peaks at 46 d and 505 d can be mistaken as planets.

Table 4. Fitted parameters for ν -Octantis and a possible planet (Ramm et al. 2009).

ν -Octantis A	
$m_A = 1.4 \pm 0.3 M_\odot$	
ν -Octantis B + planet	
$T_2 = 1050.11 \pm 0.13$ d	$T_p = 417 \pm 4$ d
$K_2 = 7032.3 \pm 2.6 \text{ m s}^{-1}$	$K_p = 51.8 \pm 1.6 \text{ m s}^{-1}$
$e_2 = 0.2359 \pm 0.0003$	$e_p = 0.123 \pm 0.037$
$\omega_2 = 75^\circ 05' \pm 0^\circ 075$	$\omega_1 = 260^\circ \pm 21^\circ$
$I_2 = 70^\circ 8' \pm 0^\circ 9$	$I_p = ?$
$\Omega_2 = 87^\circ \pm 1^\circ$	$\Omega_p = ?$
$m_B = 0.5 \pm 0.1 M_\odot$	$m_p \sin I_p = 2.5 M_J$
$a_2 = 2.55 \pm 0.13$ au	$a_p = 1.2 \pm 0.1$ au
$\sqrt{\chi^2} = 4.2$	
rms = 19 m s^{-1}	

identify as a planet with minimum mass $2.5 M_J$ and semimajor axis 1.2 au, orbiting the primary star (cf. Table 4). Moreover, the planet's period, 417 d, is nearly commensurate (ratio 2/5) with the ν -Octantis binary system's period.

A planet about halfway between the primary and secondary stars (semimajor axial ratio $\alpha = 0.47$) is unexpected. In fact, according to Holman & Wiegert (1999) the stability limit for coplanar prograde orbits around the primary star is only $a_c = 0.6$ au (equation 34). Nevertheless, Eberle & Cuntz (2010) propose that such a planet ($a_p = 1.2$ au) can be stable for at least 10 million years on a retrograde coplanar orbit.

In Table 5 we present the results of fitting the radial velocity data from Ramm et al. (2009) with a fixed Keplerian orbit (fit 0) and a precessing Keplerian orbit (fit 1). We see that fit (1) with $\dot{\omega}_2 = -0^\circ 86 \pm 0^\circ 02 \text{ yr}^{-1}$ is better than fit (0), although the difference is not yet very significant. However, as seen previously in Section 4.1, this could be due to the short observation time-span ($t_{\text{obs}} = 1.77 T_2$). In Fig. 6 we show the periodogram of the residuals after fit (0) and fit (1). After fit (0) there is a prominent signal at 417 d, while after fit (1) this signal is still present but it is no longer dominant and

⁷ Due to the Kozai effect, when $i > 40^\circ$, the inner binary's orbit cannot remain circular.

Table 5. Fits to ν -Octantis (left) and simulations I and II (right). The radial velocity data in simulations I and II were generated at the 221 observational data points for ν -Octantis, covering $t_{\text{obs}} = 5.1$ yr with a precision of about 5 m s^{-1} .

	Fit	ν -Octantis	Simulation I	Simulation II
T (d)	(1)	1050.46 ± 0.03	1114.63 ± 0.04	1093.44 ± 0.03
	(0)	1050.11 ± 0.03	1114.32 ± 0.03	1093.04 ± 0.03
	(0)+pl	417 ± 1	495 ± 2	452 ± 2
K (m s^{-1})	(1)	7044.24 ± 0.60	6895.7 ± 0.5	6970.6 ± 0.6
	(0)	7032.27 ± 0.68	6889.18 ± 0.69	6961.7 ± 0.6
	(0)+pl	51.83 ± 0.53	18.65 ± 0.69	26.2 ± 0.7
e	(1)	0.23553 ± 0.00007	0.24946 ± 0.00008	0.25388 ± 0.00008
	(0)	0.23589 ± 0.00009	0.24767 ± 0.00011	0.2524 ± 0.0001
	(0)+pl	0.124 ± 0.010	0.51 ± 0.03	0.33 ± 0.02
$\dot{\omega}$ (deg yr^{-1})	(1)	-0.860 ± 0.017	-0.500 ± 0.017	-0.810 ± 0.016
$\sqrt{\chi^2}$	(1)	7.3	2.374	3.6
	(0)	8.1	3.098	5.0
	(0)+pl	4.4	2.364	4.3
rms (m s^{-1})	(1)	36.3	13.54	19.3
	(0)	39.1	16.92	26.7
	(0)+pl	22.8	13.30	22.8

seems to be within the noise level. This is similar to the behaviour described in Section 4.3. From Table 5 we see that although fit (1) is better than fit (0), the fit with a planet at 417 d is currently better. As explained above, this could be either due to the short observation time-span or even due to the particular sampling of the radial velocity data. Moreover, the fit with the planet introduces an additional five free parameters while fit (1) introduces only one more free parameter ($\dot{\omega}_2$) which could also help to explain why the fit with the planet seems better than fit (1).

We saw that retrograde precession occurs if the secondary star in ν -Octantis is in turn a binary system inclined more than 45° with respect to the main binary's orbit (Fig. 2). In this scenario, we noted that a periodogram of the residuals left over from fitting a Keplerian orbit to the main binary could exhibit peaks that might be mistaken as planets. We saw that these peaks appeared close to harmonics of the main binary's orbital frequency. In particular, we showed an example (Section 4.3 and Fig. 4) where the fake planet's period is nearly commensurate (ratio 2/5) with the main binary's period which is exactly what happens in ν -Octantis. Therefore, we propose that a hidden binary system could mimic a planet similar to the one reported in ν -Octantis by Ramm et al. (2009).

In order to estimate inner binary parameters that lead to retrograde precession of the outer binary at a rate $\dot{\omega}_2 = -0.86 \text{ yr}^{-1}$, we set $a_1 = a_c = 0.35 \text{ au}$ (equation 34), $i = 60^\circ$ and $e_1 = 0.76$ (i.e. the inner binary is at the Kozai stationary solution). Replacing these in equations (25) and (26) with $a_2 = 2.55 \text{ au}$, $m_2 = 1.4 M_\odot$ and $m_b = 0.5 M_\odot$, we obtain estimates for the inner binary's masses of $m_1 = 0.23 M_\odot$ and $m_0 = 0.27 M_\odot$. In Table 5 we show the results of fitting a precessing Keplerian orbit (fit 1) and a fixed Keplerian orbit (fit 0) to such a triple system (simulation I). We see that fit (1) is better than fit (0) and is comparable with the fit of a planet at 495 d.

We can also estimate inner binary parameters by performing N -body fits to ν -Octantis radial velocity data. We assumed $m_2 = 1.4 M_\odot$ and fixed the outer binary's orbit at $I_2 = 70.8^\circ$ and $\Omega_2 = 87^\circ$ which are the parameters inferred from the

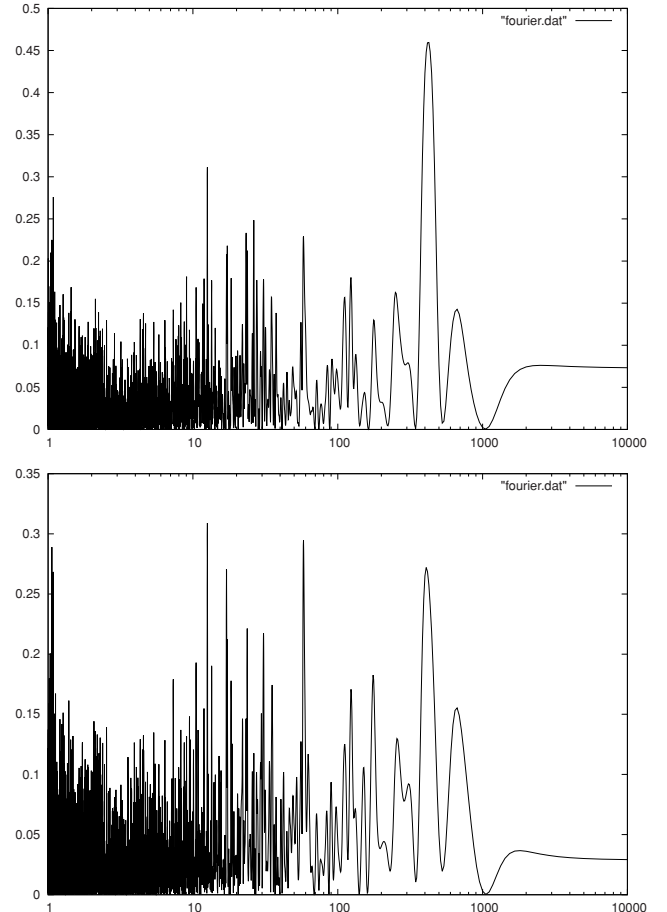


Figure 6. Fourier analysis of residuals after fit (0) and fit (1) to ν -Octantis radial velocity data (top and bottom panels, respectively).

Table 6. Best N -body fit for ν -Octantis assuming a hierarchical triple star system.

ν -Octantis A	
$m_A = 1.4 M_\odot$	
ν -Octantis B = hidden binary system	
$T_2 = 1078 \pm 1$ d	$T_1 = 189.1 \pm 1.4$ d
$K_2 = 7010 \pm 3$ m s $^{-1}$	$K_1 = 2812 \pm 76$ m s $^{-1}$
$e_2 = 0.2504 \pm 0.0003$	$e_1 = 0.67 \pm 0.03$
$\omega_2 = 72^\circ 63 \pm 0^\circ 13$	$\omega_1 = 23^\circ 25 \pm 1^\circ 38$
$I_2 = 70^\circ 8 \pm 0^\circ 9$	$I_1 = 63^\circ 4 \pm 2^\circ 7$
$\Omega_2 = 87^\circ \pm 1^\circ$	$\Omega_1 = 232^\circ \pm 1^\circ$
$m_0 = 0.496 M_\odot$	$m_1 = 0.042 M_\odot$
$a_2 = 2.565$ au	$a_1 = 0.524$ au
$\sqrt{\chi^2} = 4.9$	
rms = 25.9 m s $^{-1}$	

spectroscopic–astrometric solution (Table 4). We present the best-fitting solution in Table 6. Retrograde precession occurs because $i = 122^\circ$. Moreover, the best binary N -body fit (Table 6) is comparable to the Keplerian planet fit (Table 4). Although this solution is unstable because $a_1 \approx 1.5a_c$, we can obtain ‘equivalent’ stable configurations by reducing a_1 , while maintaining $m_b = 0.538 M_\odot$ constant, and increasing the ratio m_1/m_b , so that the Keplerian term and the quadrupole interaction term are both kept constant.

We performed a simulation of such a stable configuration with $a_1 = a_c = 0.35$ au, $m_1 = 0.109 M_\odot$ and $m_0 = 0.429 M_\odot$. In Table 5 we show the results of fitting a precessing Keplerian orbit (fit 1) and a fixed Keplerian orbit (fit 0) to such a triple system (simulation II). We see that fit (1) is better than fit (0) but fit (1) is better than the fit of a planet at 452 d. The values of the precession rate after fit (1), and both $\sqrt{\chi^2}$ and residuals (rms) after fitting the planet’s orbit, are almost equal to those obtained for the real system ν -Octantis (cf. Table 4).

From Table 5, as described above, we see that for simulated data the fit of a precessing Keplerian orbit is comparable to (simulation I) or better than (simulation II) the fit of a planet, while in the real case (ν -Octantis) the fit of a planet is currently better than the fit of a precessing Keplerian orbit. However, we stress that there are many more combinations of parameters (m_0 , m_1 , i and e_1) that can cause a precession rate $\dot{\omega}_2 = -0.86$ yr $^{-1}$, assuming that it is well constrained. Moreover, we expect our model to explain better the synthetic data generated with three-body simulations than real data (ν -Octantis) where we could have other planets or even stellar variability.

A planet around the primary star in ν -Octantis can also cause precession of the main binary’s orbit. However, our simulations show that coplanar retrograde planet orbits, as reported in Eberle & Cuntz (2010), cause slow prograde precession of the main binary’s orbit at a rate of 0.04 yr $^{-1}$. This is also what we predict from our quadrupole order theory (equations 25 and 26) although we do not expect it to be accurate at semimajor axial ratio $\alpha = 0.47$. We noted (Section 2.3) that in order to have retrograde precession, we would need the planet’s orbit to be inclined more than 45° with respect to the ν -Octantis binary. In our numerical integrations, we could not find (although we did not do an exhaustive search) stable planet orbits at semimajor axial ratio $\alpha = 0.47$ and with such high inclination with respect to the main binary.

6 CONCLUSION

We have studied the effect of a binary system on a nearby star’s motion. This complements our previous work (Morais & Correia 2008, 2011) where we assumed that we had observations for a fraction of the star’s orbit around the binary’s centre of mass. Here, we assumed that we had observations for a few orbits of the star around the binary’s centre of mass. We noted that, in this case, the secular effect of the binary dominates over the short-term effects.

We developed a secular theory which was based on a quadrupole expansion of the Hamiltonian. This is accurate for hierarchical triple systems composed of an inner binary, and a star that moves around this inner binary’s centre of mass on a wider orbit which we called the outer binary.

We derived an expression for the outer binary’s precession rate and showed that it is approximately constant. Therefore, the star’s radial velocity can be modelled as a modified Keplerian radial velocity curve with a slowly drifting amplitude. We then showed how we can measure the outer binary’s precession rate by fitting a precessing Keplerian orbit to the radial velocity data. We also showed how we can estimate inner binary parameters from the measured precession rate.

We noted that if we are unaware of the inner binary’s existence and simply fit a non-precessing Keplerian orbit to the radial velocity data, a periodogram of the residuals will show peaks at or near harmonics of the outer binary’s period which can be mistaken as planets. However, if we fit a precessing Keplerian orbit to the radial velocity data, these signals are no longer prominent in the leftover residuals. We conclude that detecting precession in the radial velocity data of a star within a binary system may be an indication that there is an unresolved third star.

We discussed the case of ν -Octantis, which is a close binary system (2.55 au) composed of a K-type star (ν -Octantis A) and a fainter companion (ν -Octantis B). Radial velocity data analysis showed a signal at 417 d which was identified as a planet at 1.2 au of ν -Octantis A. However, we showed that the radial velocity data currently implied retrograde precession of about -0.86 yr $^{-1}$ for this binary system. We suggested that this may indicate that ν -Octantis B is actually a double star which could explain a signal similar to that previously associated with a planet. At the moment we cannot yet decide that the reported planet of ν -Octantis A is simply an artefact caused by ν -Octantis B being a double star. In order to distinguish between the two hypotheses (planet or double star), we need more radial velocity data for ν -Octantis, so that we can better constrain the main binary’s precession rate. Moreover, the planet hypothesis could be compatible with retrograde precession of the ν -Octantis binary if we could prove the existence of stable orbits around ν -Octantis A, with semimajor axial ratio $\alpha = 0.47$ and inclined more than 45° with respect to the ν -Octantis binary.

ACKNOWLEDGMENTS

We acknowledge financial support from FCT-Portugal (grant PTDC/CTE-AST/098528/2008).

NOTE ADDED IN PROOF

As we were in the process of reviewing this article, we became aware of a stability study done by Goździewski et al. (in preparation) which confirms that stable planetary solutions compatible with ν -Octantis radial velocity data are unlikely.

REFERENCES

- Eberle J., Cuntz M., 2010, ApJ, 721, L168
Eggleton P. P., Kiseleva-Eggleton L., 2001, ApJ, 562, 1012
Fabrycky D., Tremaine S., 2007, ApJ, 669, 1298
Farago F., Laskar J., 2010, MNRAS, 401, 1189
Ford E. B., Kozinsky B., Rasio F. A., 2000, ApJ, 535, 385
Giuppone C. A., Leiva A. M., Correa-Otto J., Beaugé C., 2011, A&A, 530, A103
Holman M. J., Wiegert P. A., 1999, AJ, 117, 621
Kinoshita H., Nakai H., 2007, Celest. Mech. Dyn. Astron., 98, 67
Kozai Y., 1962, AJ, 67, 591
Krymowski Y., Mazeh T., 1999, MNRAS, 304, 720
Lee M. H., Peale S. J., 2003, ApJ, 592, 1201
Morais M. H. M., Correia A. C. M., 2008, A&A, 491, 899
Morais M. H. M., Correia A. C. M., 2011, A&A, 525, A152
Queloz D. et al., 2001, A&A, 379, 279
Ramm D. J., Pourbaix D., Hearnshaw J. B., Komonjinda S., 2009, MNRAS, 394, 1695
Santos N. C. et al., 2002, A&A, 392, 215
Wu Y., Murray N. W., Ramsahai J. M., 2007, ApJ, 670, 820
Zechmeister M., Kurster M., 2009, A&A, 496, 577

This paper has been typeset from a $\text{\TeX}/\text{\LaTeX}$ file prepared by the author.